Available online at www.sciencedirect.com
SCIENCE DIRECT®
Journal of Magnetism and Magnetic Materials 277 (2004) 165–174
www.elsevier.com/locate/jmmm

Preparation and radiolabeling of surface-modified magnetic nanoparticles with rhenium-188 for magnetic targeted radiotherapy

Jinquan Cao[a,*], Yongxian Wang[a,1], Junfeng Yu[a], Jiaoyun Xia[a], Chunfu Zhang[a], Duanzhi Yin[a], Urs O. Häfeli[b]

[a] *Shanghai Institute of Nuclear Research, Chinese Academy of Sciences, 2019 Jialuo Road, Shanghai 201800, PR China*
[b] *Cleveland Clinic Foundation, Radiation Oncology Department T28, 9500 Euclid Ave, Cleveland, OH 44195, USA*

Received 10 July 2003; received in revised form 22 October 2003

Abstract

Magnetite nanoparticles coated with silica were synthesized and characterized by electron microscopic methods (SEM and TEM) and crystal structure analysis (XRD). After surface modification with an amino silane coupling agent, *N*-[3-(trimethyoxysilyl) propyl]-ethylenediamine (SG-Si900), histidine was covalently linked to the amine group using glutaraldehyde as cross-linker. The magnetic nanoparticles were then radiolabeled with ^{188}Re with a labeling yield of $91.4 \pm 0.3\%$ and good stability in vitro. The labeling mechanism is suggested as fac-$[^{188}Re(CO)_3(H_2O)_3]^+$ core complexed with imidazolyl groups.

PACS: 75.50.K; 87.59.Q

Keywords: Magnetic nanoparticles; Histidine; Rhenium-188; Tricarbonyl complex; Radiolabeling

1. Introduction

Magnetic nanoparticles offer great potential applications in a variety of biomedical fields, such as improved MRI diagnostic contrast agents [1–7], cell separation [3,8–10], tumor hyperthermia [3,11–14], retinal detachment therapy [15,16], and as magnetic field-guided carriers for localizing drugs or radioactive therapies [3,10,17–19]. A silica layer on the surface of magnetic nanoparticles may be desirable because it can create a functional surface to tailor dispersibility of the nanoparticles or to form an insulating layer to control electron tunneling between particles, which may be important in charge transport or magneto-optics. In addition, the silica coating might also provide better protection against toxicity. Furthermore, it will protect the magnetite core from oxidation. A method to coat magnetite with silica was developed by Philipse in the early 1990s [20].

Alberto recently described a method to prepare the technetium (I) complex $[^{99m}Tc(OH_2)_3(CO)_3]^+$

*Corresponding author. Tel.: +862159553998289; fax: +862159558507.
E-mail addresses: cjq5@163.com (J. Cao), yongxianw@163.com (Y. Wang).
[1] Also for correspondence.

0304-8853/$ - see front matter © 2003 Elsevier B.V. All rights reserved.
doi:10.1016/j.jmmm.2003.10.022

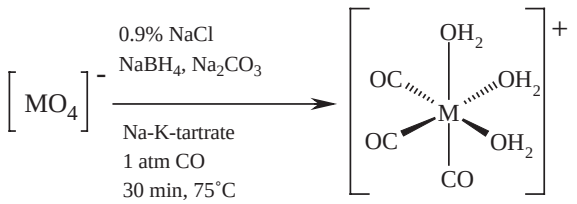

Fig. 1. Low-pressure carbonylation of $[MO_4]^-$ to obtain fac-$[M(OH_2)_3(CO)_3]^+$ (M = Tc, Re) in aqueous solution [21].

under mild conditions (Fig. 1) [21]. Whereas the carbonyls are inert, the labile water ligand can easily be exchanged by a wide variety of ligands. The fac-$[^{99m}Tc(OH_2)_3(CO)_3]^+$ does not form stable complexes with aliphatic amines and thioethers, but prefers the "soft" sp^2 nitrogen of aromatic amines. For this reason it might be an ideal candidate for labeling biomolecules such as peptides or proteins using *N*-heterocycles containing compounds as bifunctional chelating agents [22–24]. The three CO ligands are tightly bound, small, and particularly not subject to protonation which is the major competing reaction in water. In addition, as a consequence of the strong d-orbital splitting induced by the CO ligands and the d^6 electronic configuration, the complexes are of extraordinary kinetic inertness and do not exchange the ligands even in strongly competing media, forming the basis for any biological application [25]. The kinetic inertness of the +I oxidation state might also open the way for future applications of the more oxidation sensitive β^--emitting homologues of ^{186}Re and ^{188}Re for radiotherapy [26]. Rhenium-188 ($\beta^-_{max} = 2.12$ MeV (79%), 1.96 Mev (20%); $\gamma = 155$ keV (15%); therapeutic range $X_{90} = 2.1$ mm; $T_{1/2} = 16.9$ h) is an attractive therapeutic radioisotope. It is produced from decay of the reactor-produced ^{188}W parent ($T_{1/2} = 69$ d) and thus conveniently obtained on demand by elution from the ^{188}W/^{188}Re generator system [27,28].

The uptake of amino acids for protein synthesis in tumor tissue is quite rapid. Radiolabeled amino acids could thus be used in tumor imaging or radiotherapy. L-Histidine is an essential amino acid able to form stable organometallic complex with $[M(CO)_3(OH_2)_3]^+$ (M = Tc, Re) core through its imidazolyl group. (*Z*)-2-methoxyimino-2-(2-aminothiazol-4-yl)-acetic acid (**1**) and its derivates are important medical intermediates with various broad-spectrum antibiotic activities for the preparation of cephalosporins, and the thiazolyl group is a N- and S-containing heterocycle with the potential ability to chelate the $[M(CO)_3(OH_2)_3]^+$ core. Magnetic nanoparticles containing the immobilized compound (**1**) may be labeled with ^{188}Re and then used in magnetically targeted cancer radiotherapy using a magnetic force.

In this work, several surface-modified magnetic nanoparticles immobilized with histidine and compound (**1**) were prepared, and labeled with the fac-$[^{188}Re(CO)_3(H_2O)_3]^+$ core. The reaction conditions were optimized and the labeling stability tested in vitro.

2. Experimental

2-*N*-morpholinoethanesulfonic acid (MES) and $BH_3 \cdot NH_3$ were purchased from Fluka. SG-Si900 was commercially available from Nanjing Shuguang Chemical General Company. CO gas was purchased from Shanghai Ruifang Gas Co., Ltd. All other chemicals were analytical reagents and purchased from Shanghai Chemical Regents Company and used without further purification. The Nd–Fe–B permanent magnet was purchased from Shanghai Yuelong Non-ferrous Metals Co., Ltd. Carrier-free ^{188}Re-perrhenate was freshly eluted with saline from an alumina-based ^{188}W/^{188}Re-generator (Shanghai Kexing Pharm. Co., Ltd.; ^{188}W supplied by Oak Ridge National Laboratory). Particle size and morphology were measured with transmission electron microscopy (TEM) (Hitachi 600) and scanning electron microscopy (SEM) (LEO 1530 VP). The crystalline structure of the nanoparticles was characterized by X-ray diffraction (XRD), which was carried out in a *D*/max of 2550 V diffractometer using the Kα line of Cu ($\lambda = 1.5418$ Å) as a radiation source. Elementary analysis was carried out with Inductively Coupled Plasma Atomic Emission Spectrometry (ICP-AES) (IRIS Advantage 1000), a Vario EL elementary analysis instrument (Elementar, Deutch), and energy dispersive spectroscopy (EDS) attached to the SEM. Magnetic properties

were characterized in a vibrating sample magnetometer (VSM) (Model 155, EG&G Princeton Research, USA). The immobilization of histidine was confirmed by X-ray photoelectron spectra analysis (XPS) (MICROLAB-MKII, VG). The chelating efficiency was determined by thin layer chromatography (TLC) and the radioactivity monitored in a TLC scanner (AR2000, Bioscan) and γ-counter (SN-697, Shanghai Rihuan Photoelectronic Instrument Co., Ltd.).

2.1. Synthesis of magnetite nanoparticles coated with silica shell

The preparation procedure for silica-coated magnetite nanoparticles is shown in Eqs. (2.1) and (2.2). In step 1, nanomagnetite of 15 nm is formed, which is then coated in step 2 with a silica layer

$$6Fe^{3+} + SO_3^{2-} + 18NH_4OH \xrightarrow[\Delta]{N_2(g)} 2Fe_3O_4\downarrow + SO_4^{2-} + 18NH_4^+ + 9H_2O, \quad (2.1)$$

$$Fe_3O_4 \text{ magnetite} + \text{tetraethyl orthosilicate (TEOS)} \xrightarrow[EtOH-H_2O]{Base} \text{magnetite-silica}. \quad (2.2)$$

Specifically, 12 ml of a 2 M ferric chloride solution in 2 M hydrochloric acid was added to a 500-ml three-necked flask and diluted to about 100 ml with distilled water. Fifty milliliter of a freshly prepared 0.08 M aqueous sodium sulfite solution was added slowly from a funnel into the flask under bubbling with nitrogen as a protective gas. Eight milliliter of 28% ammonia diluted with 40 ml of water was then added slowly to the flask under heavy stirring and bubbling with nitrogen gas. Using a water bath, the solution temperature was kept at 70°C for 15–30 min and then cooled to below 45°C after the completion of the reaction. The black magnetite precipitate was recovered in an external magnetic field and washed several times with distilled water, followed by a water-ethanol (2:1) mixture. The precipitate was redispersed in 80 ml ethanol and 20 ml water and 5.0 ml of tetraethyl orthosilicate (TEOS) and 5.0 ml of 10 v% ammonia were added in sequence. After 12 h of stirring at 40°C, the particles were washed with methanol several times to remove unreacted TEOS and unbound silica, and finally suspended in 100 ml of methanol. A small portion of the precipitate was dried under vacuum and used for characterization.

2.2. Surface modification of silica-coated magnetite nanoparticles with amino silane (SG-Si900)

The surface modification was carried out according to Kobayashi and Matsunaga [29]. Briefly, the silane-coupling agent, SG-Si900, was added to the methanol suspension of silica-coated magnetite nanoparticles until about a concentration of 20 wt% was achieved. After about 5 min of ultrasonication in a bath type sonicator, the mixture was refluxed with stirring for above 12 h at 60°C. Unreacted SG-Si900 was removed by several washes with methanol. A small portion of the obtained precipitate was dried under vacuum and used for elementary analysis.

2.3. Immobilization of histidine and (Z)-2-methoxyimino-2-(2-aminothiazol-4-yl)-acetic acid

Histidine was immobilized on the particle surface using glutaraldehyde as cross-linker, as shown in Fig. 2. Specifically, 1 ml of SG-Si900-treated silica-coated magnetite nanoparticles dispersed in methanol (concentration >20 mg solid/ml) was extracted from the colloidal system and washed with 0.1 M phosphate buffer solution (PBS, pH 7.4). Washed particles were redispersed by ultrasonication in 1 ml of 2.5% glutaraldehyde in 0.1 M PBS (pH 7.4). After incubation at 4°C over 4 h, the suspension was centrifuged to remove the solvent and washed according to the procedure as described above. Washed particles were then redispersed in 1 ml of 0.2 M freshly prepared L-histidine solution in 0.1 M PBS-0.15 M NaCl-0.005 M EDTA (pH 7.2). After 12 h incubation at room temperature, particles were washed with 0.1 M borate buffer solution (pH 9.2) and redispersed in 0.1 M borate buffer solution (pH 9.2) containing 0.5 mg/ml $NaBH_4$ and kept at 4°C for 30 min to eliminate any unreacted aldehyde groups and double bonds. The final particles were washed

with 0.1 M PBS (pH 7.4) and finally redispersed in 1 ml of 0.5 M MES (pH 6.6).

In a separate procedure, compound (**1**) was also immobilized onto SG-Si900 modified silica-coated magnetite nanoparticles using *N*-(3-dimethylaminopropyl)-*N*′-ethylcarbodiimide hydrochloride (EDC) to activate carboxyl groups, as shown in Fig. 3. For this purpose, 1 ml of SG-Si900-treated silica-coated magnetite nanoparticles dispersed in methanol (concentration >20 mg solid/ml) was extracted from the colloidal system and redispersed in 1 ml of a freshly prepared 0.2 M (**1**)

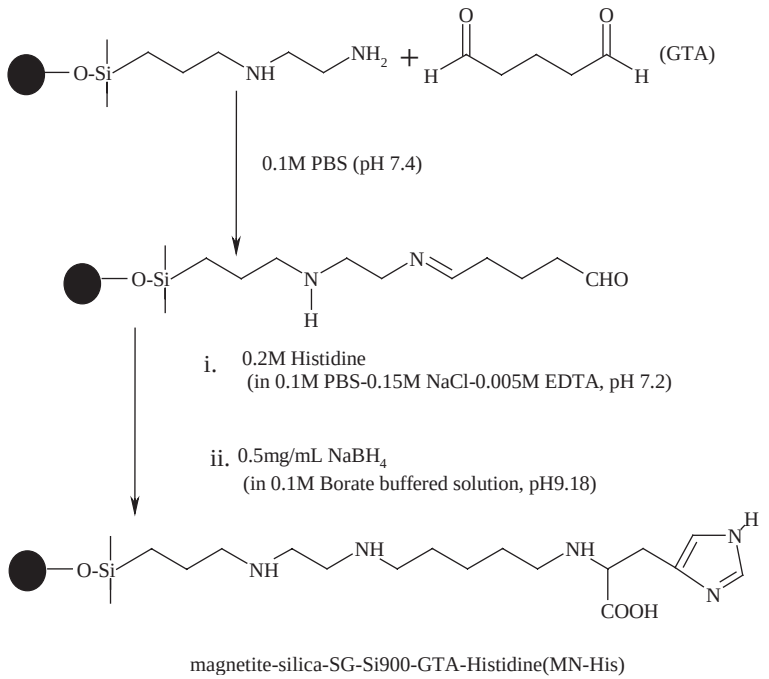

magnetite-silica-SG-Si900-GTA-Histidine(MN-His)

Fig. 2. Procedure for covalently linking histidine onto magnetic nanoparticles.

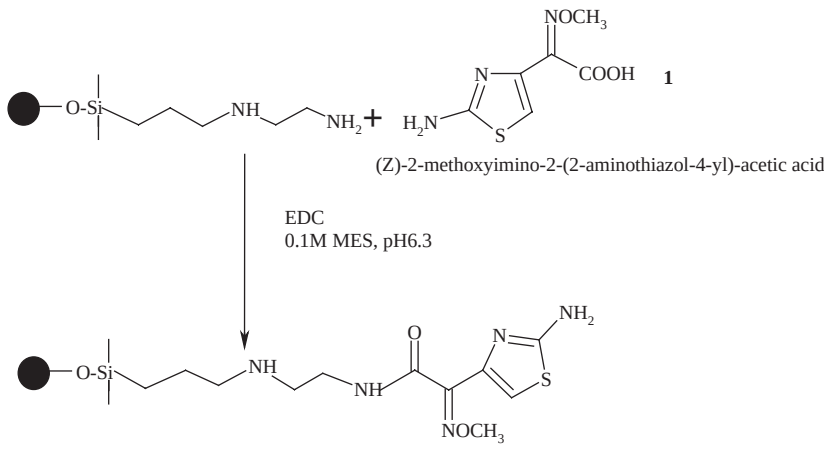

Fig. 3. Procedure for covalently linking compound (**1**) onto magnetic nanoparticles.

solution in 0.1 M MES (pH 6.3). The immobilization was started by adding 500 mg of EDC. After 12 h incubation at room temperature, particles were washed with 0.1 M PBS (pH 7.4) and finally redispersed in 1 ml of 0.5 M MES (pH 6.6).

2.4. Labeling of magnetic nanoparticles with ^{188}Re

2.4.1. Preparation of $[^{188}Re(CO)_3(H_2O)_3]$

The $[^{188}Re(CO)_3(H_2O)_3]^+$ core was prepared according to the method of Schibli et al. [26]. Five milligram of $BH_3 \cdot NH_3$ was added into a 10-ml glass vial. The vial was capped with a rubber stopper and an aluminum seal and then filled with CO gas for 20 min. The radiolabeling procedure was performed by adding the mixture of 6 μl of H_3PO_4 (85%) and 1 ml of ^{188}Re-perrhenate into the vial and incubating in a water bath at 70–80°C for 15 min. A 10-ml syringe was used to keep the balance of H_2 gas. The chelating efficiency was determined by TLC, using a SiL G/F_{254} glass plate as stationary phase and CH_3OH: hydrochloric acid (36%) = 99:1 as mobile phase. In this system, colloidal ^{188}Re stays at the origin ($R_f = 0$), the R_f of $[^{188}Re(CO)_3(H_2O)_3]^+$ is 0.4–0.6, and the free ^{188}Re-perrhenate has an R_f of 0.8–1.

2.4.2. Labeling of histidine-immobilized magnetic nanoparticles with $[^{188}Re(CO)_3(H_2O)_3]^+$ core

One hundred microliter of the above solution was added to 100 μl of magnetic nanoparticles immobilized with histidine (MN-His) dispersed in 0.5 M MES. The mixture was incubated at 60–80°C for 30–50 min. The labeled magnetic nanoparticles were extracted from the mixture using the external magnetic field of an NdFeB magnet. The radioactivity was detected in a γ-counter and the labeling efficiency calculated according to

$$\text{Labeling efficiency} = (1 - \text{radioactivity of supernatant}/\text{total radioactivity}) \times 100\%. \quad (2.3)$$

2.4.3. Stability in vitro

One milliliter of calf serum was added to the labeled magnetic nanoparticles and incubated at 37°C in a shaking water bath. The labeled magnetic nanoparticles were sampled and analyzed at 5 time points (1, 4, 24, 48, 72 h). The labeling retention stability of the nanoparticles bound ^{188}Re was then calculated according to Eq. (2.3).

3. Results and discussion

3.1. Synthesis of silica-coated magnetite nanoparticles

Magnetite nanoparticles were synthesized according to the method firstly suggested by Qu et al. [30] and silica-coated by basifying hydrolysis method. The researchers used ferrous salts as start materials with initial molar ratio of Fe^{2+}/SO_3^{2-} equal to 3 and without the use of the protective gas nitrogen in the preparation. In our experiments, we found that the reducing process was difficult to control. Furthermore, the magnetic properties of magnetic nanoparticles were rather poor without using nitrogen as a protective gas. The purity and magnetic properties of the magnetite nanoparticles were greatly enhanced if the synthesis conditions were optimized by using a theoretical initial molar ratio of Fe^{2+}/SO_3^{2-} equal to 6, nitrogen protective gas, and incubation at 70°C for 15–30 min.

3.2. Characterization of silica-coated magnetite nanoparticles

The magnetite core was characterized by XRD patterns (Fig. 4), which were consistent with crystal characteristic of magnetite (JCPDS No. 19-0629). Figs. 5 and 6 are TEM and SEM photos of silica-coated magnetite nanoparticles with an average diameter of 20 nm. The particle shape was regularly spherical. ICP analysis results confirmed the theoretically calculated concentration for silica of 24.21%, as a concentration of Fe 47.62 wt% and Si 11.32 wt% was found. The EDS analysis (Table 1) also confirmed the existence of a silica shell. Complete coating of magnetic nanoparticles with silica could be shown by XPS spectra. There was no evidence of the electronic binding energy peaks of iron (Fig. 7C). On the other hand, the

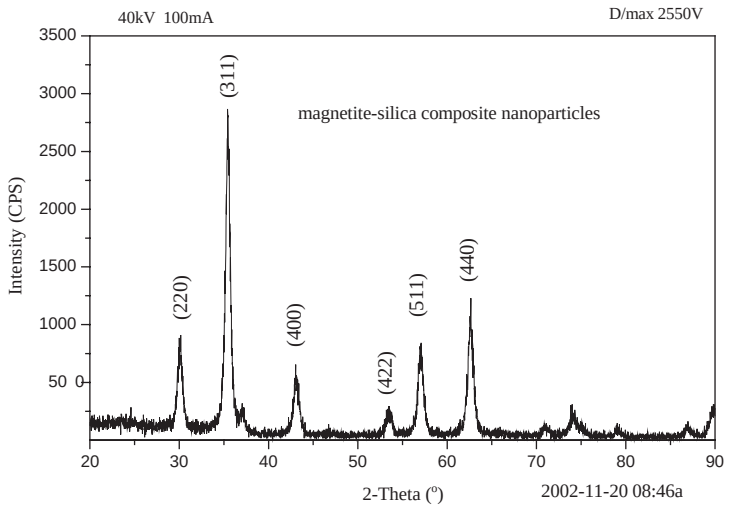

Fig. 4. XRD pattern of silica-coated magnetite nanoparticles.

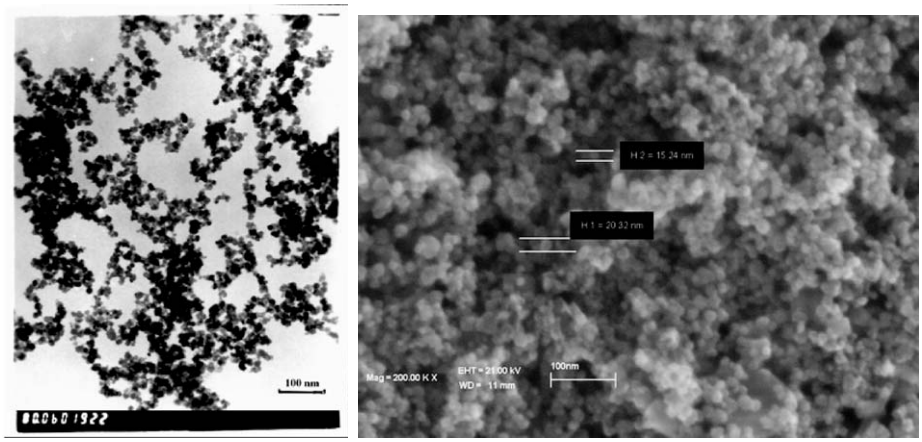

(a) (b)

Fig. 5. TEM (a) and SEM (b) of magnetite–silica nanoparticles.

electronic binding energy peaks of Si 2 s and Si 2p clearly proof the silica shell.

As the diameter of silica-coated magnetite nanoparticles is about 20 nm, which is smaller than the superparamagnetic critical size ($\sim$25 nm) [31], the nanoparticles should be superparamagnetic with zero coercivity and remanence. But in our experiment, these particles exhibited ferrimagnetic behavior with a saturation magnetization $\sigma_S = 60.9$ emu/g and a small coercivity value of $H_C = 22$ Oe. This observed ferrimagnetic behavior might be due to aggregation caused during the preparation of the sample. Our saturation magnetization values are about 33% lower than the one of bulk magnetite of 90 emu/g below 5 kOe. This is probably due to the silica layer.

3.3. Surface modification of silica-coated magnetite nanoparticles with SG-Si900

The amino group density can be calculated from the nitrogen amount measured from C, H, and N analysis of the treated magnetic nanoparticles. Elementary analysis results of silica-coated

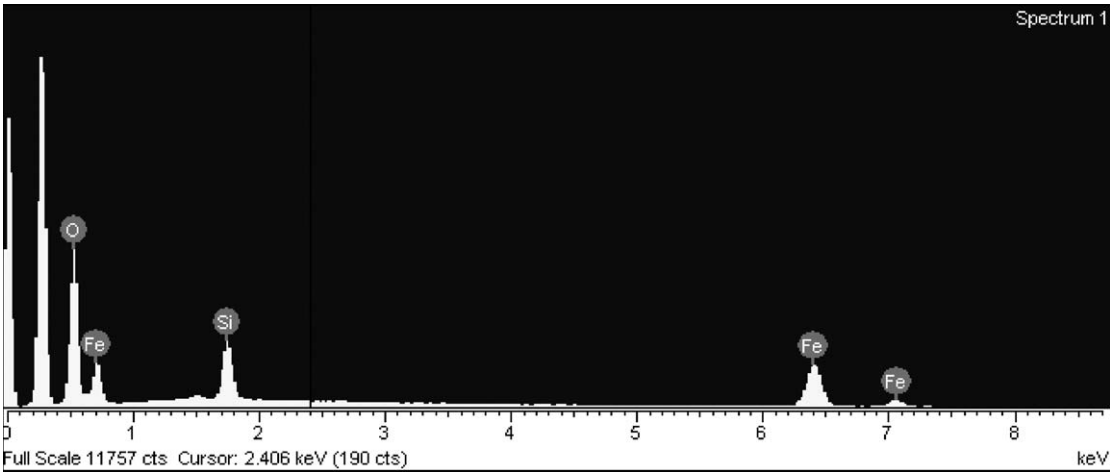

Fig. 6. EDS of magnetite–silica nanoparticles surfaces.

Table 1
Results of EDS analysis on magnetite–silica nanoparticles surfaces

Element	Weight%	Weight%	Atomic%
		Standard deviation	
O	58.08	0.48	79.01
Si	12.07	0.28	9.35
Fe	29.85	0.45	11.63
Total	100.00		

magnetite nanoparticles treated with SG-Si900 yielded 3.56 wt% C, 1.22 wt% H, and 1.55 wt% N. The amino group density is therefore about 0.5 μmol/mg solid, which is sufficient to immobilize biomolecules.

Compared to 3-aminopropyltriethoxysilane (APS), a well-known amino-functional silane coupling agent, *N*-[3-(trimethyoxysiyl)propyl]-ethylenediamine (SG-Si900) has a longer spacer arm between the alkoxysilane functionality to the inorganic support, and is more hydrophilic.

3.4. Histidine immobilization

Glutaraldehyde was used to link the amino-functional groups on the magnetic nanoparticles surface and the amino group of histidine through the Michael coupling reaction. In order to investigate the immobilization of histidine onto the magnetic nanoparticles, we have examined the MN-His and L-histidine with XPS (Fig. 7). The N1s binding energy peaks of α-amino group and imidazolyl appeared in the both, proving the immobilization of histidine onto the magnetic nanoparticles.

3.5. Labeling

The chelation efficiency of $[^{188}Re(CO)_3(H_2O)_3]^+$ was 85.7 ± 6.1% analyzed by TLC. The radiolabeling yield increased with reaction temperature up to a maximum at about 70°C (Fig. 8) and with longer reaction times up to a maximum at about 40 min (Fig. 9). A good radiolabeling yield was achieved in MES buffer at a pH range of 6.2–6.7, the optimum pH being 6.6 (Fig. 10). The ^{188}Re labeling efficiency of magnetic nanoparticles immobilized with histidine was 91.4 ± 0.3% under the optimized reaction conditions.

As a control, we also labeled SG-Si900 modified silica-coated magnetite nanoparticles without histidine on the surface, using the same optimized labeling condition. The labeling yield was 21%. This result is consistent with the fact that $[M(CO)_3(H_2O)_3]^+$ (M = Tc, Re) does not form stable complexes with aliphatic amines and thioethers, but prefers the "soft" sp^2 nitrogen of aromatic amines.

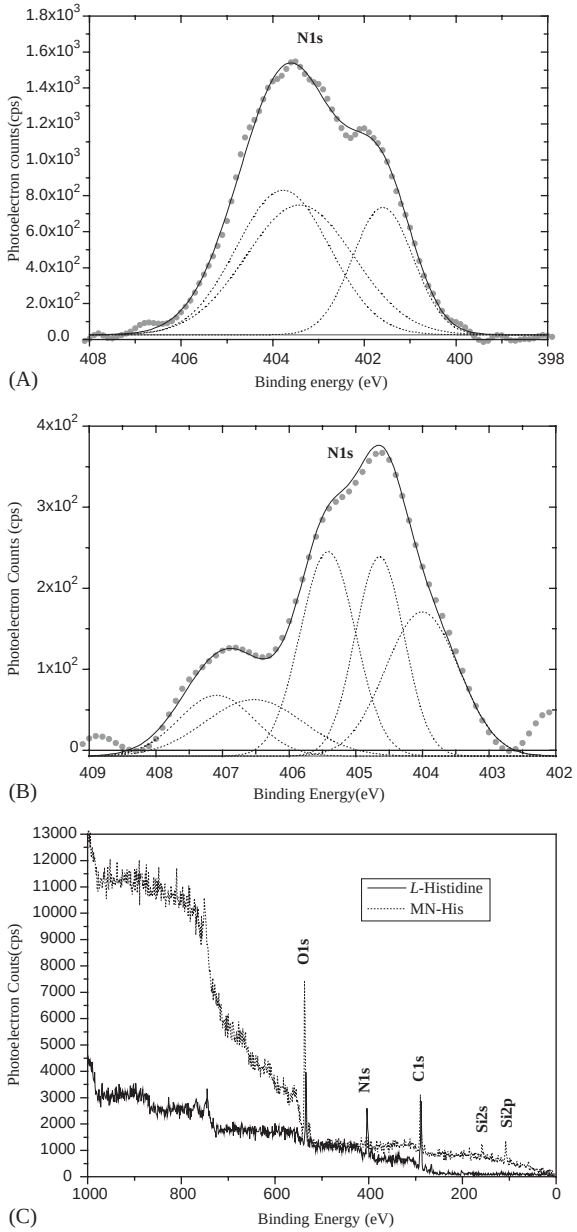

Fig. 7. XPS N1s narrow scan peak analysis of L-histidine (A) and MN-His (B); XPS-survey spectra of L-histidine and MN-His (C).

Magnetic nanoparticles with (**1**) immobilized onto their surface (MN-(**1**)) were also labeled with $[^{188}Re(CO)_3(H_2O)_3]^+$ core, reaching a lower labeling yield of $78.4 \pm 1.4\%$ compared with MN-His at the same optimized conditions.

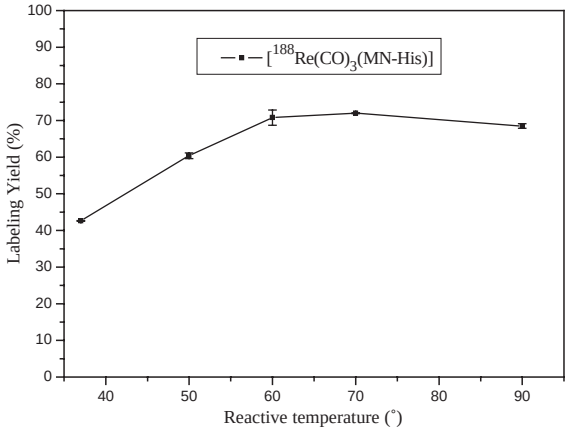

Fig. 8. Effect of reaction temperature on labeling efficiency of MN-His.

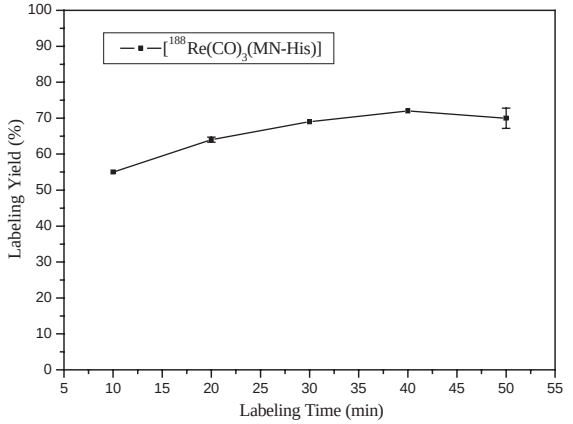

Fig. 9. Effect of reaction time on labeling efficiency of MN-His.

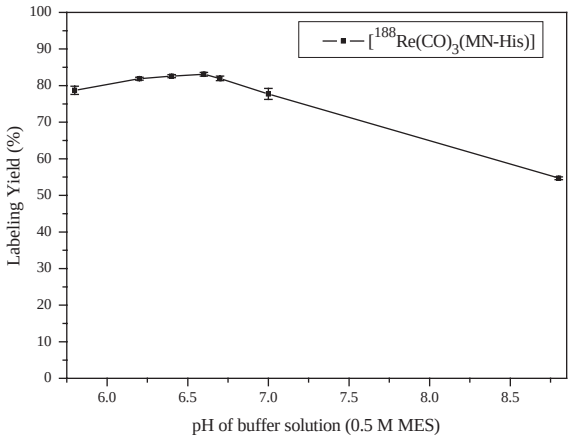

Fig. 10. Effect of pH on labeling efficiency of MN-His.

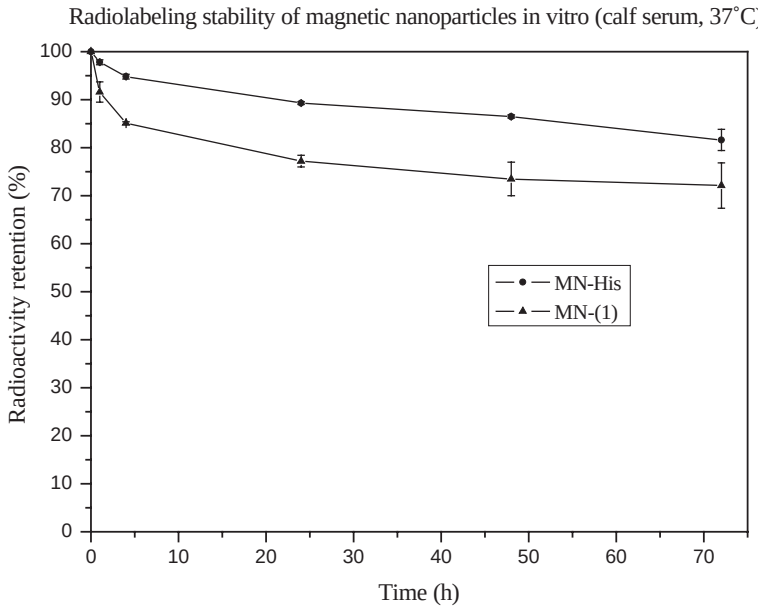

Fig. 11. Labeling stability of MN-His and MN-(**1**) in calf serum over 3 days.

All the ^{188}Re labeled magnetic nanoparticles could be stored in 0.1 M PBS (pH 7.4) for 24 h at room temperature without any evident decrease of radioactivity. In calf serum, more than 80% of radioactivity was retained by MN-His at 37°C over 3 days (Fig. 11).

MN-His is the better magnetic nanoparticle than MN-(**1**) because of its higher ^{188}Re labeling efficiency and better stability in calf serum. We are currently preparing a kit to prepare the $[^{188}Re(CO)_3(H_2O)_3]^+$ and label the MN-His. Animal studies are planned to test this magnetically targetable ^{188}Re-labeled radiopharmaceutical in the treatment of liver cancer.

Acknowledgements

We appreciate the supporting grants from Shanghai Institute of Nuclear Research (90200154, 55200321), Shanghai Municipal Committee of Sciences and Technology (0149nm.066), and Chinese Academy of Sciences (KJCX1-SW-08).

References

[1] M. Hasegawa, T. Hanaichi, H. Shoji, T. KawaguchI, S. Maruno, Jpn. J. Appl. Phys. 37 (1998) 1029.
[2] D.K. Kim, Y. Zhang, J. Kehr, T. Klason, B. Bjelke, M. Muhammed, J. Magn. Magn. Mater. 225 (2001) 256.
[3] M. Shinkai, J. Biosci. Bioeng. 94 (2002) 606.
[4] D.K. Kim, W. Voit, W. Zapka, B. Bjelke, M. Muhammed, K.V. Rao, Mater. Res. Soc. Symp. Proc. 676 (2001) Y8.32.1.
[5] M.I. Papisov, A. Bogdanov Jr., B. Schaffer, N. Nossiff, T. Shen, R. Weissleder, T.J. Brady, J. Magn. Magn. Mater. 122 (1993) 383.
[6] D.K. Kim, Y. Zhang, W. Voit, K.V. Rao, M. Muhammed, J. Magn. Magn. Mater. 225 (2001) 30.
[7] L. Babes, B. Denizot, G. Tanguy, J.J.L. Jeune, P. Jallet, J. Colloid Interface Sci. 212 (1999) 474.
[8] R.S. Molday, D. Mackenzie, J. Immunol. Methods 52 (1982) 353.
[9] S. Roath, J. Magn. Magn. Mater. 122 (1993) 329.
[10] Z. Xu, Y. Gu, WO 03/005029 A2, Canada, 2003.
[11] M. Yanase, et al., Jpn. J. Cancer Res. 8 (1986) 877.
[12] A. Jordan, R. Scholz, K. Maier-Hauff, M. Johnnsen, P. Wust, J. Nadobny, H. Schirra, H. Schmidt, S. Deger, S. Loening, W. Lanksch, R. Felix, J. Magn. Magn. Mater. 225 (2001) 118.
[13] I. Hilger, K. Frühauf, W. Andrä, R. Hiergeist, R. Hergt, W.A. Kaiser, Acad. Radiol. 9 (2002) 198.

[14] A. Jordan, R. Scholz, P. Wust, H. Schirra, T. Schiestel, H. Schmidt, R. Felix, J. Magn. Magn. Mater. 194 (1999) 185.
[15] J.P. Dailey, J.P. Phillips, C. Li, J.S. Riffle, J. Magn. Magn. Mater. 194 (1999) 140.
[16] M. Rutnakonituk, M.S. Thompson, L.A. Harris, K.E. Framer, A.R. Esker, J.S. Riffle, J. Connolly, T.G.S. Pierre, Polymer 43 (2002) 2337.
[17] K.J. Widder, et al., Proc. Soc. Exp. Biol. Med. 58 (1978) 141.
[18] K.J. Widder, G. Flouret, A.E. Senyei, J. Pharm. Sci. 68 (1979) 79.
[19] J.H. Leach, Thesis of Master of Science in Electrical Engineering, Virginia Polytechnic Institute and State University, Blacksburg, VA, 2003.
[20] A.P. Philipse, M.P.B.v. Bruggen, C. Pathmamanoharan, Langmuir 10 (1994) 92.
[21] R. Alberto, R. Schibli, A. Egli, P.A. Schubiger, U. Abram, T.A. Kaden, J. Am. Chem. Soc. 120 (1998) 7987.
[22] R. Alberto, R. Schibli, R. Waibel, U. Abram, A.P. Schubiger, Coord. Chem. Rev. 192 (1999) 901.
[23] A. Egli, R. Alberto, L. Tannahill, R. Schibli, U. Abram, A. Schaffland, R. Waibel, D. Tourwe, L. Jeannin, K. Iterbeke, P.A. Schubiger, J. Nucl. Med. 40 (1999) 1913.
[24] N. Metzler-Nolte, Angew. Chem. Int. Ed. 40 (2001) 1040.
[25] R. Alberto, R. Schibli, A.P. Schubiger, J. Am. Chem. Soc. 121 (1999) 6076.
[26] R. Schibli, R. Schwarzbach, R. Alberto, K. Ortner, H. Schmalle, C. Dumas, A. Egli, P.A. Schubiger, Bioconjugate Chem. 13 (2002) 750.
[27] F.F.J. Knapp, A.L. Beets, S. Guhlke, Anticancer Res. 17 (1997) 1783.
[28] D.Z. Yin, W.Q. Hu, X.M. Cai, J.Y. Liu, W.Y. He, W.X. Li, R. Sheng, J.F. Yu, J. Ma, J.H. Gu, Y.X. Cao, Y.X. Wang, Nucl. Tech. 21 (1998) 51.
[29] H. Kobayashi, T. Matsunaga, J. Colloid Interface Sci. 141 (1991) 505.
[30] S. Qu, H. Yang, D. Ren, S. Kan, G. Zou, D. Li, M. Li, J. Colloid Interface Sci. 215 (1999) 190.
[31] L.A. Harris, Dissertation of Ph.D. in Chemistry, Virginia Polytechnic Institute and State University, 2002.